Jurnal
Teknologi

Full Paper

EXPERIMENTAL STUDY ON UNSATURATED DOUBLE-POROSITY SOIL PHENOMENA UNDER VIBRATION EFFECT

Loke Kok Foong, Norhan Abd Rahman*, Ramli Nazir

Centre of Tropical Geoengineering, Faculty of Civil Engineering, Universiti Teknologi Malaysia, 81310 UTM Johor Bahru, Malaysia

Article history
Received
15 November 2016
Received in revised form
26 February 2017
Accepted
10 March 2017

*Corresponding author
norhan@utm.my

Graphical abstract

Abstract

A physical experiment approach was conducted to observe the deformation of double-porosity soil under vibration effect. The double-porosity soil characteristic was created using kaolin soil. An experiment on a soil sample fitted with accelerometer was conducted on a vibratory table to obtain peak ground acceleration and peak surface acceleration. After the vibration process, the deformable double-porosity soil was verified through field emission scanning electron microscopy tests. As seen in the microscope images, large surface cracks were observed due to the weakness of aggregated kaolin soil structure with its 25% water content. However, the 30% water content soil had small surface cracks due to its stronger soil structure. It was found that the deformable double-porosity soil had more fractured pores compared to the intact soil sample. From the acceleration response analysis, it was seen that both samples had amplification and dis-amplification shaking. In conclusion, the fractured double-porosity, as expected, has high permeability become a dominant factor in fluid migration. Meanwhile, the unconstrained soil and large fracture structure fabric showed significantly different porosity. The percentage of water content plays an important role in the structure of fractured double-porosity soil.

Keywords: Vibratory table, acceleration effect, water content, aggregate soil, microscope

Abstrak

Pendekatan ujikaji fizikal telah dijalankan untuk memerhati perubahan bentuk tanah liang berkembar yang mengalami kesan getaran. Tanah berciri liang berkembar telah dihasil dengan tanah kaolin. Eksperimen terhadap sample tanah dipasangkan meter pecutan dan dilaksanakan dengan mengunakan meja bergetar untuk mendapatkan pecutan bumi puncak dan pecutan permukaan puncak. Selepas proses getaran, pemboleh ubah bentuk tanah liang berkembar telah disahkan melalui ujian pelepasan medan imbasan mikroskop elektron. Dari imej mikroskop, retakan permukaan adalah besar disebabkan oleh kelemahan struktur tanah bagi kaolin agregat 25% kandungan air. Namun, 30% kandungan air yang mempunyai retakan permukaan yang kecil kerana ia mempunyai struktur tanah yang lebih kukuh. Ini adalah kerana pemboleh ubah bentuk tanah liang berkembar mempunyai keretakan liang yang lebih banyak berbanding dengan tanah liang berkembar biasa. Daripada analisis tindak balas pecutan, menunjukkan bahawa kedua-dua sampel mempunyai gegaran amplifikasi and dis-amplifikasi. Kesimpulannya, rekahan liang berkembar dijangkakan mempunyai kebolehtelapan yang tinggi dan menjadi faktor-faktor dominan dalam penghijrahan cecair. Manakala, tanah tidak dikekang dan retakan besar pada struktur fabrik menunjukkan keliangan yang ketara. Peratusan kandungan air memainkan peranan yang penting dalam struktur keretakan tanah liang berkembar.

Kata kunci: Meja bergetar, kesan pecutan, kandungan air, tanah agregat, mikroskop

1.0 INTRODUCTION

The influence of climate change and natural disasters such as el-Nino, flash floods and earthquakes were reported in Ranau and Tawau, Sabah as well as Kelantan and Terengganu [1, 2, 3, 4]. These incidents highlight that earthquake phenomenon [1, 2] has caused damage and created leaks in underground drainage pipes and water tanks. Hence, one of the greatest challenges for both professionals and researchers in Malaysia is to focus on earthquake vibrations at subsurface systems to ensure safety and protect the environment. Particularly in seismic regions, the ductility of structural material is important [5, 6, 7]. Contaminant migration in subsurface systems are partly affected by soil structure. It is well recognised that soil is typified by an abundance of soil structures at various scales that generally do not display homogeneous characteristics. Soil or rock material strength degenerates with the rise of weathering states [8, 9]. In normal circumstances, double-porosity media is soil terminology that indicates two specific scales of porous media [10]. Soils consist of two particular sub-regions with different hydraulic properties and dissimilar characteristics of pore sizes using double-porosity soil media [11]. In 2015, an earthquake in Ranau and Tawau, Sabah, Malaysia caused cracked soil porosity, unstable soil structures, soil macro structure rearrangement, and the volumetric deformation of soil aggregate structures, which affected characteristics and condition of pore sizes. Figure 1 shows a ground failure after an earthquake in Ranau, Sabah.

Figure 1 Ground failure after earthquake at Ranau, Sabah

Soil with intra-aggregate and inter-aggregate pores in well-aggregated natural soil presents a bimodal pore-size distribution found in agricultural top soils [12] and in compacted soils [13]. According to Lakeland *et al*. [14], double-porosity soil formations are from vibration effects. Saturated roughly filled granular soils such as sands and soil that are exposed to great earthquake shaking may liquefy and create large deformations with potent destructive power. Generally, in earthquake engineering, the highest response of the free surface motion is Peak Surface Acceleration (PSA) and the highest response from bedrock motion is the Peak Ground Acceleration (PGA). A PGA greater than PSA indicates dis-amplification while a PGA smaller than PSA indicates amplification, based on Eurocode 8 Part 1 for classifying ground type (A to E) and site characterisation. Projects are using vibration response analysis to model fracture soil samples, since in engineering practice, vibration response analysis is applied to identify either an amplification or dis-amplification shaking response in cracked soil. Lewandowska *et al.* [15] found in the laboratory that soil could be used to create double-porosity characteristics, leading to additional studies of double-porosity soil such as those carried out under a constant pressure head with an initial dry double-porosity medium in a series of one-dimensional infiltration experiments. Furthermore, Bagheriah *et al*. [16] performed laboratory work using prepared aggregate kaolin soil with a series of one-dimensional drying and consolidation experiments.

The existing body of research on double-porosity media focuses on rock as a media using numerical methods [17, 18, 19, 20, 21]. The previous mentioned experiments on double-porosity media have contributed knowledge and understanding of soil behaviour in double-porosity soils. Recently, numerous studies [22, 23, 24, 25, 26] using double-porosity soil media were limited to ordinary aggregated experimental and numerical models of contaminant migration in double-porosity soil that had not been subjected to earthquake effect. Experiments on fracture double-porosity soil still have a gap to realise and extend knowledge with respect to experiment on fracture double-porosity soil phenomena under vibration effects. This study provides new insights into the study of experimental vibration response analysis and verifies the fractured soil characteristics of deformable double-porosity aggregated soil.

2.0 METHODOLOGY

The details of aggregated sample preparation, experimental procedures, and setup are explained in subsequent sections.

2.1 Aggregated Sample Preparation

Kaolin soil S300 has been used to create a double-porosity soil sample. British Standard BS1377-2:1990 was used to test kaolin soil properties for the purpose of obtaining the liquid limit (41%), plastic limit (27.49%), plasticity index (13.51%), particle density (2.65Mg/m^3), and particle size distribution with silt (96%) and clay (4%). Kaolin soil is classified as silt with low plasticity (ML) under the Unified Soil Classification System (USCS) based on the value of particle size distribution, and

Atterberg limit. British Standard BS1377-4:1990 was used to obtain dry density for a 25% water content sample (1.54 Mg/m^3) and 30% water content (1.46 Mg/m^3). The compaction test curve of the soil sample is shown in Figure 2 with a maximum dry density (MDD) of 1.50 Mg/m^3 and an optimum moisture content (OMC) of 27%. The compaction process used a 2.5kg hand rammer with 3 layers and 27 blows per layer. The water content value in this experiment was 25% and 30% because the kaolin soil mixture is mouldable and the OMC was 27%. The aggregated soil sample was prepared based on the method expressed in [16] where 25% and 30% water content was mixed with dried kaolin powder to create samples 1 and 2, respectively. The soil was kept in cool condition for a minimum of 24 hours to reach water content equilibrium. Both samples were placed in a plastic bag, and the air inside the plastic bag was removed before sealing to ensure that the moisture content was maintained. Dried aggregate soil sample 1 had a bulk density of 13.75 KN/m^3 and sample 2 had a bulk density of 14.3 KN/m^3. Both samples were transposed in an acrylic soil column and compressed to a height of 100mm using a compaction machine. This study used acrylic soil columns to monitor and observe the phenomenon occurring inside the whole area of soil column. The prepared aggregate soil sample is shown in Figure 3.

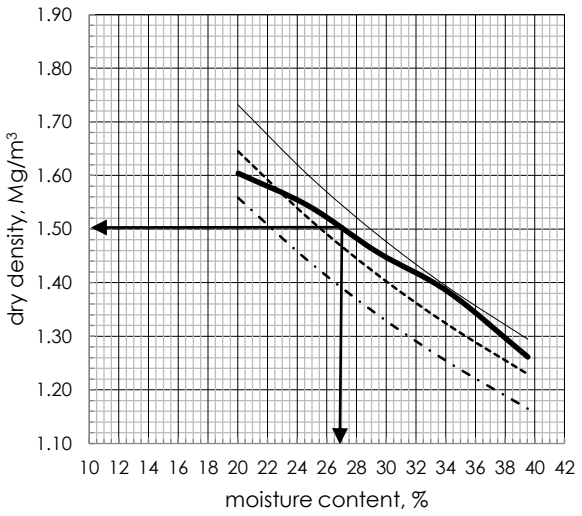

Figure 2 Compaction test curve

(a) Plan view

(b) Side view

Figure 3 Prepared aggregate soil sample

2.2 Experimental Setup and Procedure

The double-porosity characteristics of the soil samples were represented by inter-aggregate and intra-aggregate pores produced through aggregation. The deformation process used vibration during the experiment with different vibration frequencies on the soil sample concurrently to investigate fracture porous media and obtain Peak Ground Acceleration (PGA) and Peak Surface Acceleration (PSA) for both samples. The laboratory experiments were conducted in a specially designed acrylic circular soil column sealed base that is 300mm high with a 100mm outer diameter and a 94mm- inner diameter. The acrylic soil column was easy to monitor and detect the phenomenon occurring in the whole area of the acrylic soil column with an accessible experimental arrangement to accomplish this aspiration efficiently.

The acrylic soil column with a triangle base plate was placed on a vibratory table and was perfectly fixed using bolts to avoid and prevent mobility and bounce of the acrylic soil column, it is bolted on the vibratory table surface to better perceive the phenomenon occurring within the acrylic circular soil column. The experimental setup and acrylic circular soil column both reached equivalent effects using an economical

vibratory table as compared to using shake table. The actual experiment setup is shown in Figure 4.

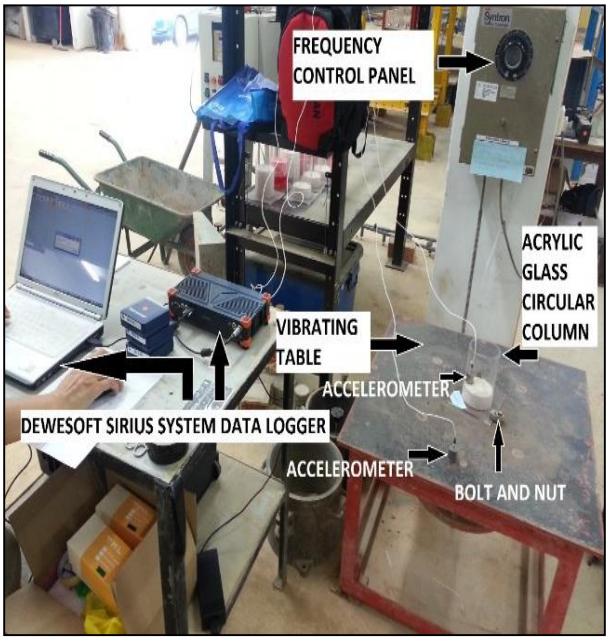

Figure 4 Actual experimental setup

The laboratory experimental setup was first arranged as shown in Figure 4. The first seismic accelerometer was installed on top of the vibratory table and the second seismic accelerometer was installed on the aggregated soil sample surface in the acrylic soil column. The installation of both accelerometers was done to obtain Peak Ground Acceleration (PGA) and Peak Surface Acceleration (PSA). The coupling system between the accelerometer and soil for PSA used soft plasticines with strong bonding behaviour, while another accelerometer for PGA has been attached to the vibratory table near the soil sample to study the near field effect. The plasticine prevented the accelerometers from being uprooted and could obtain reliable data.

Different vibration frequencies of 5Hz, 10Hz, 15Hz, 20Hz, 25Hz, and 30Hz were set using a control panel on the vibratory table to vibrate the soil sample. Prior to the experiment, to ensure that the vibratory table produced reliable testing results, the vibratory table frequencies were calibrated using a high sensitivity accelerometer together with a Dewesoft Sirius System data-logger to check and obtain excitation frequencies.

Each one of the aggregated soil sample with 25% and 30% water content were installed on top of the vibratory table and subjected to different vibration frequencies. During the vibration process, cracks that occurred in surface area were recorded using camera images. After the vibration process, a crack width microscope model 58-C0218 was used to measure the soil sample surface crack width as shown in Figure 5. The Dewesoft Sirius System data logger developed by DEWESoft was used to obtain the acceleration response of the soil sample and the vibratory table. Seismo Signal Software was used to analyse the natural frequency and vibration response of the vibration.

Figure 5 Soil sample surface crack width measurement

A scanning electron microscope was used to inspect the characteristics of soil properties [27]. The validation process for cracks appearing in the double-porosity soil under vibration was performed using a Field Emission Scanning Electron Microscope (FESEM) at 25-fold magnification, 100-fold magnification, and 500-fold magnification. Results were confirmed by coring the soil sample and visually examining the soil sample throughout its depth with a "zoomed in" image of the sample.

3.0 RESULTS AND DISCUSSION

3.1 Soil Sample Acceleration Response Analysis

The results were analysed to determine the natural frequency of the vibration. Consequently, the results for Peak Ground Acceleration (PGA), Peak Surface Acceleration (PSA), and the vibratory table calibrated natural frequency are shown in Table 1. Table 1 shows that the vibratory table calibrated natural frequency was distinguished from the frequency at the vibratory table control panel as previously mentioned. Therefore, the natural frequency was used as the vibratory table frequency obtained from the calibrated high sensitivity accelerometers. The result from Table 1 were used to natural frequency plot graphs versus PGA and PSA.

Table 1 Results of vibratory table natural frequency, PGA and PSA

Calibrated Vibratory Table Natural Frequency (Hz)	Acceleration (m/s²)	
	Sample 1 (PSA / PGA)	Sample 2 (PSA / PGA)
0.29	10.56 / 06.98	04.34 / 05.96
0.34	09.62 / 08.12	04.86 / 07.76
0.39	09.78 / 09.95	10.34 / 09.50
0.49	09.12 / 12.31	14.89 / 11.65
0.68	10.37 / 16.16	12.57 / 16.04
0.98	05.54 / 22.47	14.30 / 22.84

Figures 6 and 7 present the graphs for natural frequency versus PGA and PSA for sample 1 (25% water content) and sample 2 (30% water content), respectively. As can be seen in Figure 6, fractures started to appear due to the vibration process (acceleration), which began at a frequency of 0.29Hz. Figure 6 shows the fractured double-porosity amplified shaking due to the loosening of the soil, which experiences greater seismic shaking compared to compacted soil at the area before the intersection point at frequencies between 0.29Hz to 0.39Hz. The process of dilation started to take place since the soils internal force started to uplift the aggregated soil samples at the intersection point that occurred at 0.39Hz. Beyond the intersection point, the graph displays dis-amplified values, which do not reflect actual PSA values because the accelerometer was disconnected from the soil surface area due to the terrible fracturing and dilation process. Based on Eurocode 8 Part 1: 2004 + A1: 2013 for the identification of ground types, sample 1 had a ground type D as a soft-to-firm cohesive soil because soil sample 1 has amplification shaking during the vibration process.

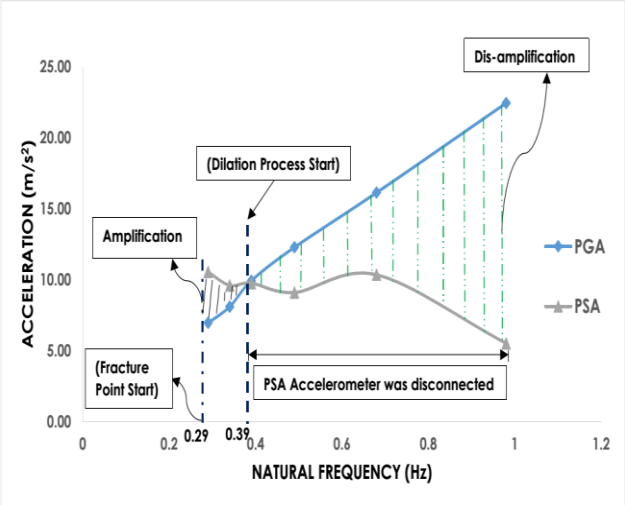

Figure 6 Graph of natural frequency versus PGA and PSA for sample 1

Figure 7 shows two intersections of PSA and PGA at 0.39Hz and 0.58Hz. The area before the first intersection point, 0.39Hz, displays dis-amplified shaking for soil sample 2 because the soil is still intact and it experienced lesser seismic waves compared to soft soil and loose soil at the frequency before 0.39Hz. The first intersection point occurred at 0.39Hz where fractures started to occur in the aggregated kaolin. The area between the first intersection and second intersection shows amplified shaking because the soil started to loosen and weaken. The graph 7 showed that the aggregated kaolin started to re-compact due to great vibration force in the boundary condition phenomena, even though the surface still showed fractures at 0.58Hz in the area after the second intersection point. Based on Eurocode 8 Part 1: 2004 + A1: 2013 for the identification of ground types, sample 2 had a ground type B as it was a very stiff soil that displayed dis-amplification shaking and re-compaction of the soil sample. Soil sample 2 with a water content of 30% was very close to the 27% Optimum Moisture Content (OMC) for kaolin soil. This study found that based on the acceleration response analysis, the fractured / cracked in sample 1 was greater in effect and occurred earlier due to soil stiffness and plasticity [28]. Stiffer and low plasticity index which less than 15% material tend to experienced higher brittleness compared to sample 2. Sample 1 experienced more seismic shaking during the vibration process until the soil sample was uplifted.

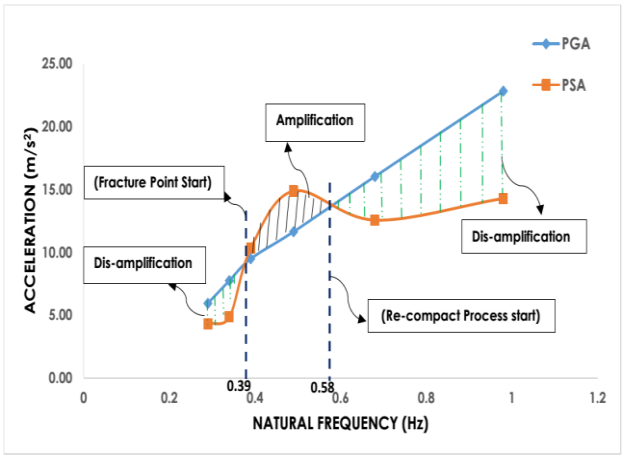

Figure 7 Graph of natural frequency versus PGA and PSA for sample 2

3.2 Soil Sample Characteristics Validation

Figure 8 reveals the results before and after surface cracking for sample 1 and sample 2. The differences between sample 1 and sample 2 after the vibration process are clearly highlighted. Based on the results generated by the crack width microscope, surface crack widths are large for samples with 25% water content, while 30% water content samples displayed small surface cracks. The correlation between sample 1 and sample 2 is significant because fracture and cracking patterns are obvious. Sample 1 has larger cracks compared to sample 2 that has only a small crack. The findings of this study add to a growing body of literature on double-porosity soil experiments. Ngien *et al.* [11] and Sa'ari *et al.* [23] performed undamaged double-porosity soil experiments. Compared to this study, results indicate that the vibrated double-porosity soil has larger pores and fractured surfaces. Crack patterns show that water content plays an important role because a difference of only 5% water content has a significant effect on the soil sample surface.

(a) Sample 1 with 25% water content before vibration

(b) Sample 1 with 25% water content after vibration

(c) Sample 2 with 30% water content before vibration

(d) Sample 2 with 30% water content after vibration

Figure 8 Result of before and after vibration for sample 1 and sample 2

Figure 9 shows the result of depth zoomed in image of the vibrated double-porosity samples with 25% and 30% water content at 500-fold magnification. The fractured kaolin granules were magnified to 500-fold indicate its intra-aggregate pores. Soil sample surface fractures and fine inter-aggregate pores were perceived in resultant FESEM test at 25-fold magnification and at 100-fold magnification, respectively. Based on the results of the FESEM test, this study found that the fractured double-porosity of the soil sample was verified with deformable characteristics such as fractured aggregate double pores, inter-aggregate double pores, and intra-aggregate pores, which indicate that the soil structure had undergone rearrangement and had fractured double-porosity after the vibration process. The evidence results of the FESEM test are clearly seen in the case of 25% water content sample, as aggregated kaolin has a fine soil granule structure in which the soil is a mix of shapes ranging from flat to moderate spheres compared to the 30% water content aggregated kaolin that had a coarse soil granule structure in which the soil exhibits polyhedral and crumb shapes. Furthermore, based on the FESEM results, both samples had a granular soil structure because the soil fragments of both samples had diameters less than 0.5cm. Therefore, the characteristics of deformable double-porosity soil that experienced the vibration process were verified by the FESEM test. The fractured and cracking of the soil sample surface is predicted to lead to quicker liquid migration in subsurface systems.

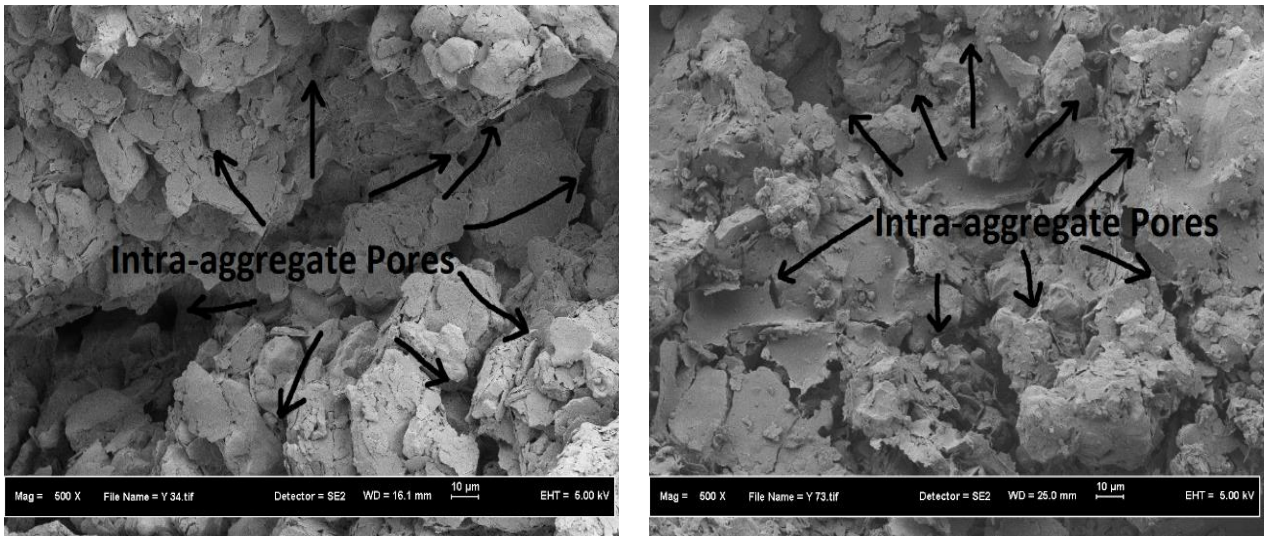

(a) 25% water content (b) 30% water content

Figure 9 FESEM zoom in image of vibrated double-porosity with 500-fold magnification

4.0 CONCLUSION

This research was purposely designed to determine the effect of vibration responses and to verify the fractured soil characteristics of deformable double-porosity aggregated soils with different water contents. This study strengthens the idea that soil samples with low water content has caused the fracture process to appear faster, even with very slow ground acceleration, as well as high Peak Surface Acceleration (PSA); however, in this study, the result was inverse with high water content. Furthermore, density and water content influenced the crack / fractures of sample 1 and 2. Soil fracturing was due to macro-micro structure bonding interactions. One of the more significant findings to emerge from this study is that the percentage of water content plays an important role because differences in water content show obvious surface cracking results. In addition, a FESEM test at 500-fold magnification clearly showed that aggregated soil sample 1 had a coarse-grained structure. In contrast, aggregated sample 2 had a flaky-grained structure. Thus, fractured double-porosity with coarse-grained structures and flaky-grained structures are expected to be factors affecting fluid movement in subsurface systems.

Hence, the evidence from this study suggests that samples with 30% water content are the best mixture for kaolin soil because of its small surface cracks, smaller seismic shaking, and stronger soil structure based on Eurocode 8 Part 1: 2004 + A1: 2013 and is very close to the 27% Optimum Moisture Content (OMC) for kaolin soil.

Acknowledgement

This study was supported by the Research Management Centre (RMC), Universiti Teknologi Malaysia under Research University Grant – Tier 1

(PY/2016/06547). The authors would also like to thank the Engineering Seismology and Earthquake Engineering Research Group (eSEER), UTM. The first author was supported through a Federal Training Award by the Public Service Department under the Prime Minister's Department, Malaysia.

References

[1] Muguntan, V., Ruben, S., and Stephanie, L. 2015, June 5. Strong Earthquake Strikes Sabah. *The Star Online*. From http://www.thestar.com.my/news/nation/2015/06/05/sabah-quake/. Retrieved 12th November 2015.

[2] Stephanie, L. 2015, Dec 22. Tawau Residents Shaken by Quake. *The Star Online*. From http://www.thestar.com.my/news/nation/2015/12/22/tawau-residents-shaken-by-quake-early-morning-tarakan-temblor-sends-people-running-out-of-homes/. Retrieved 21th Jan 2016.

[3] Pour, A. B., and Hashim, M. 2016. Geological Features Mapping Using Palsar-2 Data in Kelantan River Basin, Peninsular Malaysia. *The International Archives of the Photogrammetry, Remote Sensing and Spatial Information Science,Volume XLII-4/W1, International Conference on Geomatic and Geospatial Technology, 2016. Kuala Lumpur, Malaysia.* 3-5 October 2016. 65-70.

[4] Randhawa, S. S. 2016, Nov 29. Flash Floods Hit Terengganu. The Star Online. From http://www.thestar.com.my/news/nation/2016/11/29/flash-floods-hit-terengganu/. Retrieved 2nd Feb 2017.

[5] Ma, C. K., Awang, A. Z., and Omar, W. 2014. Slenderness Effect and Upper-Bound Slenderness Limit of SSTT-Confined HSC Column. *International Journal of Structural Engineering*. 5(3): 279-286.

[6] Ma, C. K., Awang, A. Z. and Omar, W. 2016a. Flexural Ductility Design of Confined High-Strength Concrete Columns: Theoretical Modelling. *Measurement*. 78: 42-48.

[7] Ma, C. K., Awang, A. Z., Garcia, R., Omar, W., Pilakoutas, K. and Azimi, M. 2016b. August. Nominal Curvature Design of Circular HSC Columns Confined with Post-tensioned Steel Straps. *Structures*. 7: 25-32.

[8] Liang, M., Mohamad, E. T., Khun, M. C. and Alel, M. N. A. 2015a. Estimating Uniaxial Compressive Strength of Tropically Weathered Sedimentary Rock Using Indirect Tests. *Jurnal Teknologi*. 72(3): 49-58.

[9] Liang, M., Mohamad, E. T., Komoo, I. and Chau-Khun, M. 2015b. Performance Evaluation of Existing Surface Excavation Assessment Methods on Weathered Sedimentary Rock. *Bulletin of Engineering Geology and the Environment*. 76(1): 205-218.

[10] Carminati, A., Kaestner, A., Lehmann, P., and Fluhler, H. 2008. Unsaturated Water Flow across Soil Aggregate Contacts. *Adv. Water Resource.* 31: 1221-1232.

[11] Ngien, S. K., Rahman, N. A., Bob M. M., Ahmad, K., Sa'ari, R., and Lewis, R. W. 2012. Observation of Light Non-Aqueous Phase Liquid Migration in Aggregated Soil Using Image Analysis. *Transport in Porous Media*. 92(1): 83-100.

[12] El-Zein, A., Carter, J. P., and Airey, D. W. 2006. Three-Dimensional Finite Elements for the Analysis of Soil Contamination Using a Multiple-Porosity Approach. *International Journal for Numerical and Analytical Methods in Geomechanics.* 30: 577-597.

[13] Li, X., and Zhang, L. M. 2009. Characterization of Dual-Structure Pore-Size Distribution of Soil. *Canadian Geotechnical Journal.* 46: 129-141.

[14] Lakeland, D. L., Rechenmacher, A., and Ghanem, A. 2014. Toward a Complete Model of Soil Liquefaction: The Importance of Fluid Flow and Grain Motion. *Proc. R. Soc. A.* 470: 20130453.

[15] Lewandowska, J., Szymkiewicz, A., Gorczewska, W., and Vauclin, M. 2005. Infiltration in a Double-Porosity Medium: Experiments and Comparison with a Theoretical Model. *Water Resources Research.* 41: W02022.

[16] Bagherieh, A. R., Khalili, N., Habibagahi, G., and Ghahramani, A. 2009. Drying Response and Effective Stress in a Double Porosity Aggregated Soil. *Engineering Geology.* 105: 44-50.

[17] Valliappan, S., and Khalili-Naghadeh, N. 1990. Flow through Fissured Porous Media with Deformable Matrix. *International Journal for Numerical Methods in Engineering.* 29: 1079-1094.

[18] Bourgeat, A., Luckhaus, S., and Mikelic, A. 1996. Convergence of the Homogenization Process for a Double-Porosity Model of Immiscible Two-Phase Flow. *SIAM Journal on Mathematical Analysis.* 27(6): 1520-1543.

[19] Pau, W. K. S., and Lewis, R. W. 2002. Three-dimensional Finite Element Simulation of Three-Phase Flow In A Deforming Fissured Reservoir. *Comput. Methods Appl. Mech. Eng.* 191: 2631-2659.

[20] Ryzhik, V. 2007. Spreading of a NAPL Lens in a Double-Porosity Medium. *Computational Geosciences.* 11: 1-8.

[21] Ngien, S. K., Rahman, N. A., Ahmad, K., and Lewis, R. W. 2012. Numerical Modelling of Multiphase Immiscible Flow In Double-Porosity Featured Groundwater Systems. *International Journal of Numerical and Analytical Methods in Geomechanics.* 36: 1330-1349.

[22] Ngien, S. K., Rahman, N. A., Ahmad, K., and Lewis, R. W. 2012. A Review of Experimental Studies on Double-Porosity Soils. *Scientific Research and Essays.* 7(38): 3243-3250.

[23] Sa'ari, R., Rahman, N. A., Abdul Latif, H. N., Yusof, Z. M., Ngien, S. K., Kamaruddin, S. A., Mustaffar, M., and Hezmi, M. A. 2015. Application of Digital Image Processing Technique in Monitoring LNAPL Migration in Double-Porosity Soil Column. *Jurnal Teknologi.* 3(72): 23-29.

[24] Kamaruddin, S. A., Sulaiman, W. N. A., Rahman, N. A., Zakaria, M. P., Mustaffar, M., and Sa'ari, R. 2011. A Review of Laboratory and Numerical Simulations of Hydrocarbons Migration in Subsurface Environments. *Journal of Environmental Science and Technology.* 4(3): 191-214.

[25] Lewandowska, J., Ngoc, T. D. T., Vauclin, M., and Bertin, H. 2008. Water Drainage in Double-Porosity Soils: Experiments and Micro-Macro Modelling. *Journal of Geotechnical and Geoenvironmental Engineering.* 134(2): 231-243.

[26] Loke, K. F., Rahman, N. A., and Ramli, M. Z. 2016. A Laboratory Study of Vibration Effect for Deformable Double-Porosity Soil with Different Moisture Content. *Malaysian Journal of Civil Engineering*. Special Issue 28(3): 207-222.

[27] Hayden, N. J., and Voice, T. C. 1993. Microscopic Observation of a NAPL in a Three-Fluid-Phase Soil System. *Journal of Contaminant Hydrology.* 12: 217-226.

[28] Alonso, E. E., Gens, A., and Josa, A. 1990. A Constitutive Model for Partially Saturated Soils. *Géotechnique*. 40(3): 405-430.